Journal of Scientific Research and Development 2 (3): 177-182, 2015
Available online at www.jsrad.org
ISSN 1115-7569

A new method to calculate mathematical morphology using associative memory and cellular learning automata

Ali Azimi Kashani *, Alimohamad Monjezi Nori, Iman Mosavian

Department of Computer Engineering, Shoushtar Branch, Islamic Azad University, shoushtar, Iran

Abstract: The methods presented in this paper include using auto-associative memory which can be defined as a supervised organizing method which is a specific type of h-sorting which is compatible with the morphologic operators over multi-variables data. Mathematical morphologies for multi-variable images require appropriate sort descriptions that allow us to define and use primitive morphologies operators without any wrong results such as wrong color. All the required calculations are defined with lattice algebra (+,^ and ∨); therefore, the proposed method will be faster with less computation overhead than the previous methods. This method does not use any assumptions of the stochastic process which means that this method is independent of the model. The presented method uses cellular learning automata which results in fewer errors than the mathematical methods due to the feedback from the network.

Key words: Biometrics; Eye tracking; Identity verification; Eye detection

1. Introduction

Mathematical morphology was presented by J. Serra (Serra, 1984) J. Serra (1988)) and P. Maragos (Matheron, 1975)) as a strong tool for image processing. During past fifty years, mathematical morphology has shown capabilities in different areas such as image processing and machine vision; or in different applications such as segmentation of the medical images, remote sensing grouping, noise cancelation, tissue analysis and detecting geometrical shapes. Morphologic operation consists of mapping between complete meshes which are represented with $\mathbb{L}$ or $\mathbb{M}$. These sets are partially ordered that for each pair, the infimum and supermum are defined. Erotion and dilation are two basic morphologic operators. Let us consider data from rs-fMRI for these operators are divided into healthy characters (HC), schizophrenia with or without audio disorder (SZAH and AZnAH respectively). The goal is to find different brain network patterns in these groups. Using cellular learning automata for clustering in order to search for the low frequency components in brain, performs lattice calculation which is equivalent to the dependent or independent component analysis for fMRI steady state analysis. A BOLD voxel time series can be used to build a lattice auto-associative memory. This process will also be applied to the remaining voxels of the 4D fMRI data. In this case, the h-function illustrates the similarity of the brain operations. Input data of the h-function are extracted from the cellular learning automata which can be stabilized with appropriate feedback and minimum iterations. After detecting the brain networks, the operational relations in the brain can be observed by thresholding the brain information map. This process can be done using morphologic operators that can extract specific features from the data.

1.1. Multi-variable sorting

Since Morphologic operators perform well over the scalar images. However, it is difficult to apply these operators over multi-variable images until a vector space is defined to conserve the natural characteristics of the morphologic operators. For example, one important characteristic of these operators is that the results of the erosion and dilation stay in the range of the image and no new color is generated. Proposed methods in (Barnett, 1976), I. Pitas and P. Tsakalides (1991), E. Aptoula and S. Lefevre (2007)) are some examples of the multi-variable ordering that suffer from generating new colors. One solution to this problem is to use reduced ordering (J. Angulo.(2007), S. Velasco-Forero and J. Angulo(2011))

$$x \leq_h y \Leftrightarrow h(x) \leq h(y);\ \forall x, y \in X \quad (1)$$

Discounted sorting can be defined based on a supervised classification. This classification system, the extracted values of some pixels are trained and bred. The separator function values or the analog values that are used for classes assessment, defines h mapping. The normalization is presented in(S. Velasco-Forero and J. Angulo (2011)) , sorting supervised h on the set X, is a sort of h which satisfies conditions $h(b) = \bot, \forall b \in B$, $h(f) = \top, \forall f \in F$ somehow $B, F \subset X$ are subset of X which $B \cap F = \emptyset$ and $\bot$ and $\top$ are respectively, the upper and lower elements of the destination network. Abrasion

* Corresponding Author.

operators increases areas of the image that are close to the background and expanded operations increase the areas that are close to the foreground. Since h functions are not necessarily One-to-one, h sorting results may not present a general schema. While we need to distinguish among members of classes, $\ell[z] = \{c \in \mathbb{R}^n | h(c) = z\}$, our factor for disambiguation is lexical sort of them.

1.1.1. Multivariate morphological operators

For a multivariate image $\{I(p) \in \mathbb{R}^n\}_{p \in D_I}$, while D_I is the image space, and taking into consideration the structural object S, supervised Abrasion operation h is defined: $\varepsilon_{h,s}(I)(p) = I(q)\, s.t.\, I(q) = \bigwedge_h \{I(s): s \in S_p\}$ which in $\bigwedge_h$ is the largest lower bound which is concluded from increased sorting $\leq_h$ from equation(1). S_p is an structural element which is defined in P pixel location. Also, we have expanded supervised operation h which is defined $\delta_{h,s}(I)(p) = I(q)\, s.t.\, I(q) = \bigvee_h \{I(s): s \in S_p\}$ which in $\bigvee_h$ is the smallest higher bound based on equation (1). Morphological gradient for images with scalar values, computed as the difference between the wear and stretch the image I S and is defined by structural elements: $g_S(I) = \delta_S(I) - \varepsilon_S(I)$. In multivariate images, supervised morphological gradient h, likewise abrasion supervised h means $\varepsilon_{h,S}(I)$ and dilation $\delta_{h,S}(I)$ defined as:

$$g_{h,S}(I) = h\left(\delta_{h,S}(I)\right) - h(\varepsilon_{h,S}(I)) \quad (2)$$

LAAM h mapping as Chebyshev distance is defined between main pattern vector and calling resulted LAAM. In [10] this distance is used as an agent for nearest neighbor classification based on lattice. In our schema, this distance is used as supervised classification agent. If $x \in \mathbb{R}^n$ would be a sample data vector and $X = \{x_i\}_{i=1}^K$, $x_i \in \mathbb{R}^n$ as a non-empty training set, for all $i = 1, \dots, K$, LAAM h mapping calculates following:

$$h_X(c) = d_c(x^{\#}, x) \quad (3)$$

Which in $x^{\#} \in \mathbb{R}^n$ is dilated response to the input vector x as: $x_M^{\#} = M_{XX} \,\overline{\wedge}\, x$. Also we can use abrasion memory calling W_{XX} as $x_W^{\#} = W_{XX} \,\overline{\vee}\, x$. Function $d_c(a,b)$ points to Chebyshev distance between two vectors that using the largest absolute difference between the components of the vector is calculated as: $d_c(a,b) = \bigvee_{i=1}^n |a_i - b_i|$

1.1.2. H mapping

If we have training set X, a foreground supervised sorting, which is showed by $\leq_X$, is defined based on h mapping in (3) equation as following:

$$\forall x, y \in \mathbb{R}^n, x \leq_X y \Leftrightarrow h_X(X) \leq h_X(y) \quad (4)$$

Foreground supervised sorting, produce a complete lattice $\mathbb{L}_X$ which correspond lower element $\perp_X = 0$ with fixed node set M_{XX} and W_{XX}. It means $h(x) = \perp_X$ for any $x \in \not\Vdash(X)$. Hence, higher element is equal to $\top_X = +\infty$.

1.1.3. Foreground/Background h mapping

For creating a supervised Foreground/Background h mapping, we need training set B for foreground and training set F for background separately. H mapping which is defined in equation (4) operates in data by means of F and B training set. So, h_B and h_F are resulted. As a result, we make a foreground/background h mapping with combination of $h_B$and h_F to an h mapping and named it $h_r(x)$:

$$h_r(x) = h_F(x) - h_B(x) \quad (5)$$

Where the value of it for $x \in \not\Vdash(B)$ will be positive and for $x \in \not\Vdash(F)$ will be negative. Therefore, we use this function as a separator where as $h_r(x) > 0$ points to foreground class pixels and $h_r(x) < 0$ points to background class pixels. For every points where $h_r(x) = 0$ are considered as the boundary decision. Supervised h sorting shows $\leq_r$ and defines:

$$\forall x, y \in \mathbb{R}^n, x \leq_r y \Leftrightarrow h_r(x) \leq h_r(y) \quad (6)$$

Mapped of Foreground/background h mapping is a complete lattice $\mathbb{L}_r$which lower and higher elements of it are $\perp = -\infty$ and $\top = +\infty$ respectively. The h Mapping do not correspond to standards presented in(S. Velasco-Forero and J. Angulo(2011)), because for $b \in B$ we have $h_r(b) \neq \perp$ and also for $f \in F$ we have$f \in F$, although, resulted sorting and morphology operators presents acceptable results.

2. Learning automata

Automaton is an abstract object that can perform a limited number of actions, each action done by the environmental risk assessment and response to the automaton. Automaton based on this response, chooses the next action. During this process, the automaton learns to select the best action. The way of using response to the environment, in which the automaton used to select the next action, defines by Algorithm learning automaton.

A learning automata is composed of two parts: A stochastic automata with a limited number of action and a random environment that is associated with the automaton. Automata learning algorithms that learn to lie in the use of the optimal operation. In the proposed method, color information in YCBCR environment and Gaussian mixture model has been used. Since the region above the eyebrows and below the eyes is brighter, the eye region is cropped. This region, which starts above the eyebrows and extends to the region below the eyelids, includes two eyebrows, two eyes, and their characteristic parts like eyelids and eye corners. Applying bag of pixels method, we roughly locate the pupil. Having identified the pupil in the initial frame, we detect the eye region by kallman filtering.

2.1. Random Automata

For math description of a random automata, a five-member set $SA \equiv \{\alpha, \beta, F, G, \phi\}$ are used.

$\alpha \equiv \{\alpha_1, \alpha_2, \ldots, \alpha_n\} \equiv$ Actions set of automata

$\beta \equiv \{\beta_1, \beta_2, \ldots, \beta_n\} \equiv$ Inputs set

$F \equiv \phi \times \beta \rightarrow \phi \equiv$ The function maps the current state to new state by using appropriate response of environment.

$G \equiv \phi \rightarrow \alpha \equiv$ Output function that maps current states to output

$\phi_{(H)} \equiv \{\phi_1, \phi_2, \ldots \phi_k\} \equiv$ Internal states automata in H moment

α set includes output automata which select it from this set in one stage out of r. β input set determine input of automata.When F and E functions are determined, we called automata: Deterministic Automata. In this situation, with having automata, current state and input, it can be concluded next state and output. Whenever F and G functions are randomly, we call it Random Automata. In this situation, we can just show the probability of next situation and next input of the automata. Random Automates are two types: A: Random Automata with fixed structure. B: Random Automata with variable structure. In the first one, the probability of operation of automata is fixed while in the second one these probabilities are shown in every stage.

2.2. The Scales of behavior of learning automata

Two main factors n automata efficiency are initial states and probability of punishing from environment. The initial states could be vector of probability of initial operation of punishing probability are usually non-defined. Hence in some application we know them.

2.2.1. Cellular Automata

Cellular Automata are actually discrete dynamical systems behavior based solely on a local basis. In cellular automata, a space is defined as a network in which every house is called a cell. Cellular automata can also be considered as computational systems that process information coded in them. The cellular automata with a control unit can be interpreted as an SIMD machine.

2.2.2. Cellular Learning Automata

Cellular learning automata, where each cell is composed of cellular automata to one or more of the automata equipped. The output is applied to each cell state automaton. Cellular automata rule will determine whether the selected action by cellular automata should be rewarded or penalized. Reward or penalty for causing the cellular structure learning automata is defined in order to achieve a defined goal. Cellular learning automata can be used in various structures of the neighborhood

Fig. 1: Different neighborhood

Cellular learning automata can be expressed as follows: In every moment of every LA in cellular learning automata selects an action from the set of his actions. This can be based on previous or randomly selected learning automata based on vector operations. Selected to act according to the law governing the exercise of choice by neighboring cells and cellular learning automata, are rewarded or penalized. Depending on the response, Learning automata have corrected their behavior in this way; it will update its internal structure. This is usually done for all cells simultaneously. Action selection process and the reward or penalty until the system reaches a steady state or a pre-defined criteria to be used lasting. Fig. 2 shows the cellular learning automata in which the von Neumann neighborhood is used. In this way, they are happy Atvmatahayy before Atvmatahayy rewards and penalties that have been upset before.

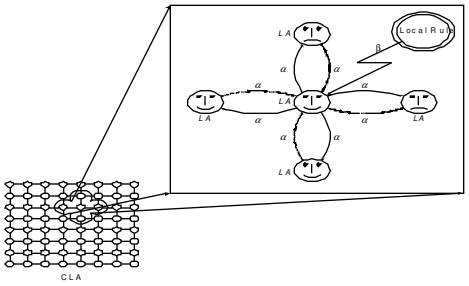

Fig. 2: Cellular learning automata (CLA)

Terms of cellular learning automata into three general categories, holistic and divided the total foreign-oriented. In spite of this general rule, the amount is not individual cells. But in general terms the value of a cell based on a next step, the number of neighboring cells are different depending on modes. In spite of this general rule, the amount is not individual cells. The only difference in the rules of the foreign-oriented laws are generally oriented in the next cell in the specified amounts, in addition to the current state of the neighboring cells of the cell, the current state of the cell effective it is.

3. The proposed method is evaluated and patterns

In this section we report two experiments that have been performed on rs-fMRI data provided. In the first experiment, a group analysis based on patterns of each group has done. In this analysis, we calculated the mean of each group space rs-fMRI data, then to have identified networks of cellular learning automata are used to obtain an appropriate threshold for networks of brain function. In the first experiment, (a) for each of the next four recorded

data are averaged to create models, (b) all parts of the brain processed the data, (c) its focus on mapping function h Foreground / Background leave, (d) According to that in (Ann K. Shinn, Justin T. Baker, Bruce M. Cohen, and Dost Ongur, (2013)) is a network derived from a specific location in the brain evaluated and, (e) threshold cellular automata networks with feedback surveys to determine the function of each class of our population. Work on population patterns, allows us to assess the impact on the group level, which are evident in the data mean we evaluated. In a second experiment, we provide the results of the classification for each category of the population. In this category, the specifications given in this way gain: First, create a mapping function h supervised sorting provides discounted to the left lateral Heschl's gyrus. Pearson correlation coefficient between values of h function and variable related to each classification for each voxel let us to determine more informative voxels. Although this way decrease the processing speed because of its computation costs. We try to create a profile vectors by selecting cellular automata to automata and by placing additional assumptions that increase the number of states per cell and the neighboring variables over time in these sites by using the values of the function h. The results obtained based on K-NN dividers show that, this way could make accurate differentiation between [different] populations cause.

3.1. Results of tests on rs-fMRI

In these section results of tests on fMRI fixed data are expressed which in from 28 healthy persons (NC) and two groups of Schizophrenia which 26 of them have hearing problems (SZAH) and 14 cases without it (SZnAH) are selected. We articulate following definitions for comparing with previous methods:

Tanimoto coefficient: Tanimoto coefficient uses for calculating the similarity networks has been found suitable for the use in order to limit the use of our networks. If we consider two sets A and B, Tanimoto coefficient of similarity of the two as the cardinality of the community expressed their subscription:

$$T(A,B) = \frac{|A \cap B|}{|A \cup B|} \quad (7)$$

This respect, the degree of overlap between the two sets of measurements. Tanimoto coefficient is normal into T∈ [0,1] range. If there is no resemblance T = 0 and T = 1 will be in full compliance. When comparing the results of image segmentation, image collections will be the same areas.

Pearson Coefficient: Pearson correlation coefficient is calculated as follows:

$$r = \frac{n(\sum xy) - (\sum x)(\sum y)}{\sqrt{[n\sum x^2 - (\sum x)^2][n\sum y^2 - (\sum y)^2]}} \quad (8)$$

Where $r \in [-1,1]$ and $r = 1$ means perfect correlation between two variables, and $r = -1$ means perfect negative correlation between the two series. In this issue, the Pearson correlation between pre-resulted class labels and fMRI neural connections are evaluated by function h**.**

3.2. First test

After performing preprocessing step, we calculate the Z series for each voxel. The images were normalized to calculate the mean BOLD (blood oxygen level dependent) among individuals in each group use. Finally, the mean dimensional in healthy subjects, schizophrenic disorder and schizophrenia, we calculate the noise patterns corresponding to each of them to create. Based on the results in(Ann K. Shinn, Justin T. Baker, Bruce M. Cohen, and Dost Ongur (2013)), the objective of this experiment was to determine the status of the network associated with a particular voxel in the left transverse temporal gyrus (LHG coordinates and -26 and 10 MNI -42) is located. This situation is shown in Fig. 3. Since our goal is to identify the effects of hearing impairment, particularly in the auditory brain. MNI coordinates of the pattern data are extracted from each group. We use the map function h according to foreground / background on every model we have calculated. In this case, the voxels in the images 3 and 4, respectively, have identified it as training set foreground and background used**.**Voxel background sets with LHG (transverse temporal gyrus, left) and voxel background sets with CSF (spinal fluid) in a match that ventricle [Collections] corresponding time series are noisy or irrelevant. Calculation function h foreground / background, a map with the actual values on brain volume that can be applied to a threshold on this mapping, functional brain networks identified. We want to consider the threshold somehow the difference between networks from each group would be highest and simultaneously the size of founded networks (which called them voxel) would be largest. Finding this threshold in the first stage is similar to previous methods but with adding a learning automata the threshold decreased by 5%. At a first glance this amount of decrease may not effect to computations but various tests by means of cell automata resulted maximum amount in decrease at running time. However, previous approaches for calculating the threshold h mapping in identified brain areas that apply in different patterns, calculated the coefficient Tanimoto coefficient between those areas. In fact that we are dealing with complex voxels which depends on threshold applied to mapping h function. Therefore, $X(\theta)$ is voxel sets with threshold of h function on them are higher than θ value. Therefore we have: $T(\theta) = T(X(\theta), Y(\theta))$. We are seeking distinct areas which are brain networks that are unique for each population group. So what should find Tanimoto coefficient with small values for regions (networks) of the brain with considerable size (large).

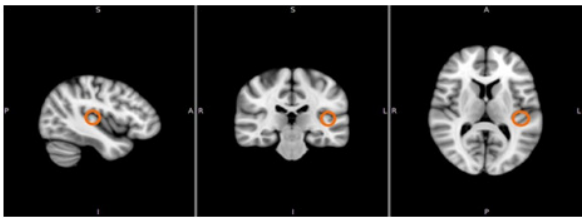

Fig. 3: Foreground voxel seed site from the left Heschl's gyrus (LHG; -42,-26, 10)(Darya Chyzhyk,(2013))

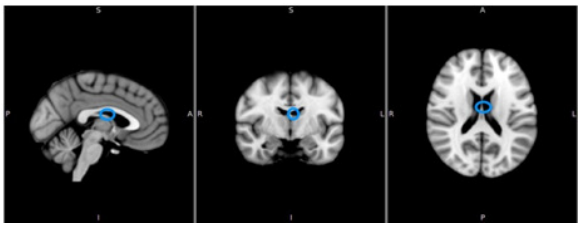

Fig. 4: Background voxel seed site from CSF of the ventricle. (Darya Chyzhyk, (2013))

Fig. 5 shows two graphs. The first graph of pair wise similarities population networks which by increasing a factor of Tanimoto coefficient threshold and value $T(\theta)$ has measured. Consider the similarities of healthy subjects (HC) in the two groups, rather than two other unhealthy ones are more the same. Also, Tanimoto coefficient have high amount considerably which shows those two groups are common in many features. Nonetheless, we seek to make a difference in the separation / classification to help us. Given that each cell selects a limited number of available positions, it is possible to significantly increase the degree of similarity, therefore, we focus on smaller quantities: For $\theta > 0.7$ the Tanimoto coefficient $T(\theta)$ for both healthy and sick groups is almost zero, meaning that the network almost discrete (a few common features). In proposed method, we at the beginning assumed to be discrete. Comparing between two sick groups whenever $\theta > 0.8$, Tanimoto coefficient is close to zero. The second graph is related to size of networks which determine by the number of voxel sets. It can be seen that for $\theta > 0.7$ size of network are going to be too small, so, the amount of $\theta > 0.7$ are selected as a threshold for following images. Fig. 6 shows results of classification results based on the difference between pair-classes: Healthy subjects in comparison to patients without hearing problems (HC vs. nAH), with hearing problems (HC vs. AH). Colored bars shows the size of features which produce because of voxels with the highest Pearson Coefficient. In all cases, classification efficiency for high sized vectors is increased. The best result are given by comparing healthy subjects to patients without hearing problems which shows we can distinct this sort of patients better rather than healthy subjects.

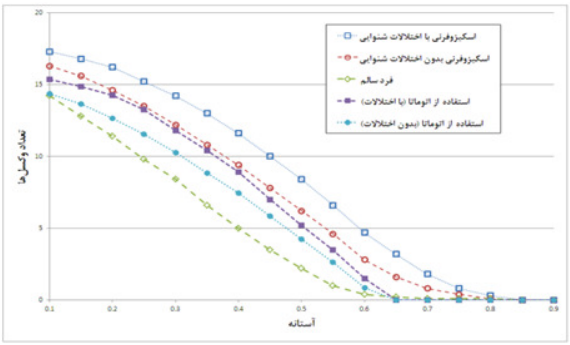

(a)

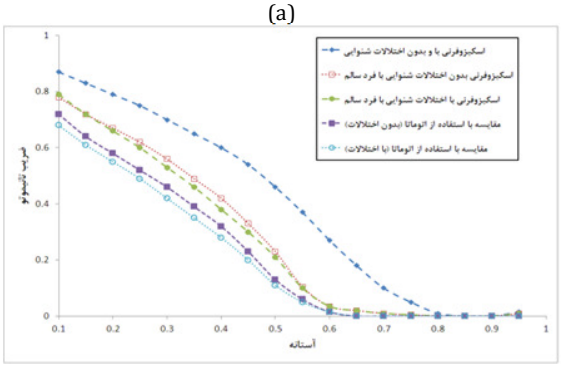

(b)

Fig. 5: Effect of threshold value on the identified networks on back-ground/foreground h-function brain map. (a) Tanimoto Coefficient comparing net-works from each pair of population, and (b) size of the detected clusters

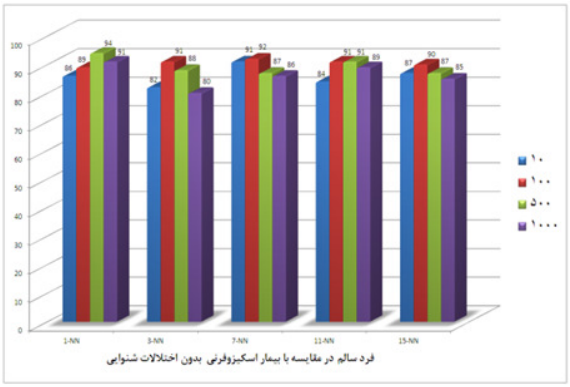

(a)

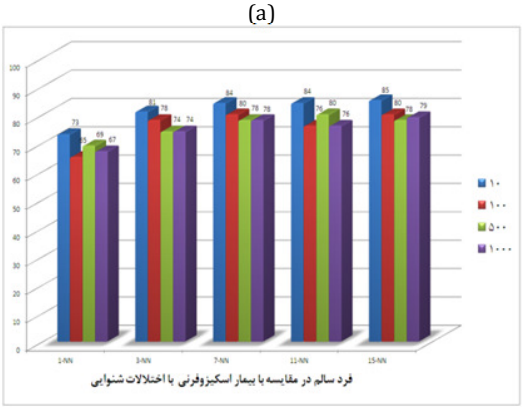

(b)

Fig. 6: Maximum Classifier Accuracy found in 10 repetition of 10-fold cross validation for k-NN classifier k = 1; 3; 7; 11; 15. The bar colors represent different number of extracted features.

4. Conclusion

In this paper, a supervised Foreground / Background sorting of cellular learning automata approach was proposed. The main advantage of it is the stability and compatibility of the morphological operators and filters. The proposed method for analyzing fMRI data is needed to define the set of voxels. Of course, any of the assumptions and statistical techniques is not used in this method. In general, this method is independent of the model. This idea produce much more error rather than others mathematical methods Considering that cell updating is a synchronizing action and rules are not accidental and also a rule in each site just depends on neighbors' values, and the idea that rule for new value of each site depends on limited number of previous states. For rs-fMRI, the result of the test to detect differences between brain networks in schizophrenia patients who are hearing impaired and those that do not interfere offered that we may be the location for the extracted index profile voxel help. In the first experiment, the brain networks by placing a limit on the mappings h were calculated. This mapping is calculated using the appropriate threshold function h using learning automata are done. Networks that were detected obvious differences between the population [of] their own, and this allows distinguishing among people based on an individual basis and using the classification. Supervised background / foreground h mapping on rs-fMRI, provide properties to determine the potential cause schizophrenia and calculate the Pearson correlation coefficient by analog variable make difference between individuals with and without hearing impairment. Depending on what the indicators presented in the previous method in terms of classification accuracy of the profile vectors derived from the choice of evaluated voxel sets. However, the computational costs are higher than our method, therefore the automata results are very accurate, especially in separating normal subjects and patients with hearing impairment, results can be achieved by applying classification complex data.

References

Ann K. Shinn, Justin T. Baker, Bruce M. Cohen, and Dost Ongur. Functional connectivity of left heschl's gyrus in vulnerability to auditory hallucinations in schizophrenia. Schizophrenia Research, 143(2-3):260 – 268, 2013**.**

Barnett. The ordering of multivariate data. Journal Of The Royal Statistical Society Series A General, 139(3):318–355, 1976.

Darya Chyzhyk, "Contributions of Lattice Computing to Medical Image Processing", theses, Universidad del País Vasco Euskal Herriko Unibertsitatea Donostia - San Sebastian 2013.

E. Aptoula and S. Lefevre. A comparative study on multivariate mathematical morphology. Pattern Recogn., 40(11):2914–2929, November 2007.

G. Matheron. Random sets and integral geometry. Wiley series in probability and mathematical statistics: Probability and mathematical statistics. Wiley, 1975.

I. Pitas and P. Tsakalides. Multivariate ordering in color image filtering. IEEE Transactions on Circuits and Systems for Video Technology, 1(3):247– 259, 295–6, September 1991.

J. Angulo. Morphological colour operators in totally ordered lattices based on distances: Application to image filtering, enhancement and analysis. Comput. Vis. Image Underst., 107(1-2):56–73, July 2007.

J. Serra. Anamorphoses and function lattices. volume 2030, pages 2–11.SPIE, 1993.

J. Serra. Image Analysis and Mathematical Morphology, Vol. 2: Theoretical Advances. Academic Press, 1st edition, February 1988.

J. Serra. Image Analysis and Mathematical Morphology, Volume 1 (Image Analysis & Mathematical Morphology Series). Academic Press, February **1984**

S. Velasco-Forero and J. Angulo. Supervised ordering in Rp: Application to morphological processing of hyperspectral images. IEEE Transactions on Image Processing, 20(11):3301–3308, November 2011.